



Universiteit
Leiden
The Netherlands

Exploration of the endocannabinoid system using metabolomics

Di, X.

Citation

Di, X. (2023, February 7). *Exploration of the endocannabinoid system using metabolomics*. Retrieved from <https://hdl.handle.net/1887/3515754>

Version: Publisher's Version

License: [Licence agreement concerning inclusion of doctoral thesis in the Institutional Repository of the University of Leiden](#)

Downloaded from: <https://hdl.handle.net/1887/3515754>

Note: To cite this publication please use the final published version (if applicable).

Chapter 4

Plasma levels of endocannabinoids and their analogues as potential markers of cardiometabolic risk in young adults

Based on

Xinyu Di*, Borja Martinez-Tellez*, Elke H.J. Krekels, Lucas Jurado-Fasoli, Francisco J. Osuna-Prieto, Lourdes Ortiz-Alvarez, Amy C. Harms, Jose V. Garcia-Lario, Thomas Hankemeier, Patrick C.N. Rensen, Jonatan R. Ruiz, Isabelle Kohler

Plasma levels of endocannabinoids and their analogues as potential biomarkers of cardiometabolic risk in young sedentary adults

Submitted.

*authors contributed equally

ABSTRACT

Background and aim: The endocannabinoid system (ECS) is a signalling system composed of endocannabinoids (eCBs), their receptors, and the enzymes involved in their synthesis and metabolism. Alterations in the ECS are linked to the development of cardiometabolic diseases. Here, we investigated the relationship between plasma levels of eCBs and their analogues with body composition and cardiometabolic risk factors.

Methods: The study included 133 young adults (age 22.1 ± 2.2 years, 67% women). Fasting plasma levels of eCBs and their analogues were measured using liquid chromatography-tandem mass spectrometry (LC-MS/MS). Body composition, brown adipose tissue (BAT) volume, and FDG uptake, as well as traditional cardiometabolic risk factors, were measured.

Results: Plasma levels of eCBs and several eCB analogues were positively correlated with adiposity and traditional cardiometabolic risk factors (e.g., serum insulin and triacylglycerides levels, all $r \geq 0.17$ and $p \leq 0.045$). Plasma levels of 2-AG and PDEA were negatively correlated with BAT volume and glucose uptake (all $r \leq -0.17$ and $P \leq 0.047$). We observed that the plasma levels of eCBs and their analogues were higher in metabolically unhealthy overweight-obese (MUOO) participants compared to metabolically healthy overweight-obese (MHOO) participants.

Conclusion: Our findings suggest that the plasma levels of eCBs and their analogues can be used as potential markers of cardiometabolic risk in young adults.

Keywords: body composition, cardiometabolic risk factors, anandamide, endocannabinoid system, 2-arachidonoyl glycerol, visceral adipose tissue.

1. INTRODUCTION

Cardiometabolic diseases (CMD) are the leading cause of mortality worldwide^{1,2}. The increase in obesity and obesity-related cardiometabolic disorders, including dyslipidemia, hyperglycemia, hypertension, and abdominal fat accumulation partially drives the increments in the prevalence of CMD^{3,4}. Despite the recent advances in understanding the pathological mechanisms underlying the onset and progression of CMD, additional efforts to further improve the prognosis and diagnosis of these diseases are required.

An attractive and potentially effective strategy for the early diagnosis of CMD is the use of lipid mediators as markers. The endocannabinoids (eCBs) anandamide (AEA) and 2-arachidonoyl glycerol (2-AG) are the endogenous agonists of the cannabinoid receptor type 1 (CB1R) and type 2 (CB2R)⁵. These two receptors, together with the eCBs and their metabolic enzymes, compose the endocannabinoid system (ECS), which plays a significant role in, amongst others, energy balance⁵. Several clinical studies have shown alterations in the ECS in patients with CMD⁶⁻⁹ but led to inconsistent findings concerning the role of AEA and 2-AG in CMD, which highlights the need for further studies. Not only the eCBs seem to be important in CMD, but also their structural analogues¹⁰, which include N-acyl ethanolamines (NAEs), such as N-palmitoylethanolamine (PEA), N-oleoylethanolamine (OEA), and N-linoleylethanolamine (LEA), as well as other 2-acylglycerols, such as 2-linoleoylglycerol (2-LG) and 2-oleoylglycerol (2-OG). These structural homologues do not have affinity for CB1R or CB2R but can enhance the effects of AEA and 2-AG on their receptors by increasing their affinity or inhibiting their hydrolysis (so-called *entourage effect*)^{11,12}.

Overall, several studies have suggested that eCBs and their analogues may be potential biomarkers for CMD⁶⁻⁹. These studies were focused on middle-aged or elderly populations, while the potential to use these metabolites as CMD biomarkers in younger populations has not been investigated. Therefore, in this study, we aimed to investigate the association of plasma levels of eCBs and their analogues with body composition parameters and cardiometabolic risk factors in a cohort of young adults.

2. MATERIAL AND METHODS

2.1. Study design and participants

This cross-sectional study was performed under the framework of the ACTIBATE study (ClinicalTrials.gov, ID: NCT02365129)^{13,14}. The study included 136 young adult participants, 45 males and 91 females (**Table 1**). All participants were recruited via advertisements in electronic media and leaflets. The inclusion criteria included an age of 18 to 25 years; being engaged in less than 20 min of moderate or vigorous physical activity per day on <3 days/week; not smoking; having a stable body weight over the past three months (change <3 kg); without any CMD (e.g., hypertension, diabetes); not taking any medication that might affect cardiovascular function; and no history of cancer among first-degree relatives.

2.2. Determination of plasma levels of endocannabinoids and endocannabinoid analogues

Plasma levels of AEA, 2-AG, and their analogues (i.e., 2-LG, 2-OG, N- α -linolenoyl ethanolamine (alpha-LEA), N-dihomo-gamma-linolenylethanolamine (DGLEA), N-docosahexaenylethanolamine (DHEA), LEA, OEA, PEA, N-pentadecenylethanolamine (PDEA), N-palmitoleylethanolamine (POEA), and N-stearoyl ethanolamine (SEA)), together with arachidonic acid (AA), i.e., a downstream metabolite of AEA and 2-AG, were assessed using liquid chromatography-tandem mass spectrometry (LC-MS/MS) after liquid-liquid extraction (LLE). The LLE-LC-MS/MS method has been described previously^{15,16}. Deuterated internal standards (listed in **Table S1**) were used to correct for analytical errors. Quality control (QC) samples were regularly injected during the measurements and used to evaluate the data quality and correct for between-batch variations using the in-house developed mzQuality workflow (available at <http://www.mzQuality.nl>)¹⁷. Relative standard deviations (RSDs) were calculated for each analyte present in the QC samples using the peak area ratios (i.e., peak area of the target analyte divided by the peak area of the respective internal standard). Metabolites with RSDs $\leq 15\%$ were included in further data analyses. Metabolites showing RSDs higher than 30% on peak area ratios in QC samples were excluded. Metabolites with $15\% \leq \text{RSDs} < 30\%$ were interpreted with caution (**Table 1**). The experimental procedure is detailed in the **Supplementary Material**.

2.3. Anthropometry and body composition

Body weight and height were measured using a SECA model 799 electronic column scale and a stadiometer (SECA, Hamburg, Germany). The waist circumference was measured in the minimum perimeter, at the end of a normal breath expiration, with the arms relaxed on both sides of the body. The measurements were taken just above the umbilicus following a horizontal plane when the minimum perimeter could not be detected, such as in overweight or obese participants. The waist circumference was measured twice with a plastic tape measure, and the two measurements were averaged. Lean body mass (LBM), fat body mass (FBM), and visceral adipose tissue (VAT) were determined with a Hologic Discovery Wi dual-energy X-ray absorptiometer (Hologic, Marlborough, MA, USA). Body mass index (BMI), lean mass index (LMI), and fat mass index (FMI) were calculated by dividing body weight, LBM, and FBM (in kg) by the square of the height (in m), respectively. The fat mass percentage (%) was calculated as the FBM divided by total body mass and multiplied by 100.

2.4. Activation and determination of ¹⁸F-fluorodeoxyglucose uptake by brown adipose tissue

Activation of brown adipose tissue (BAT) was carried out using a personalized cooling protocol for each participant on two independent days. This personalized cooling protocol has been extensively described elsewhere¹⁸. Briefly, we first determined the shivering threshold of each participant; 48-72h later, the uptake of ¹⁸F-fluorodeoxyglucose (¹⁸F-FDG) by BAT was determined. During the shivering threshold test, participants were exposed for 30 min to a warm room for acclimation purposes, before moving to a mild-cold room. Next, participants wore a water-perfused cooling vest (Polar Products Inc., Stow, OH, USA) during the second part of the test. The water temperature of this cooling vest was reduced from 16.6 °C to ~2.2 °C per 10 min until participants began shivering. 48-72 h later, the participants went to the hospital, where they were exposed to the same cooling protocol for 2 h at ~4 °C above the water temperature, for which they reported shivering. A sub-group of individuals did not report shivering and were therefore exposed to the lowest water temperature of the device. After 1 h of cold exposure, a bolus of ~185 MBq of ¹⁸F-FDG was intravenously injected, before positron emission tomography/computed tomography (PET/CT) scan (Siemens Biograph 16 PET/CT, Siemens Healthcare, Erlangen, Germany)

2 h later. The BAT volume and BAT ^{18}F -FDG activity were determined following standard guidelines¹⁹ using the Beth Israel plugin for the FIJI program. This required the determination of the number of pixels in the region of interest with a radiodensity range of -190 to -10 Hounsfield Units, as well as the individualized, standardized threshold ^{18}F -FDG uptake values (SUV) [$1.2/(\text{LBM}/\text{body mass})$]¹⁹. BAT volume was determined as the number of pixels in the range described above, with an SUV value above the SUV threshold. BAT metabolism activity was determined concerning the mean SUV (SUV_{mean}, i.e., the mean quantity of ^{18}F -FDG contents in three pixels within a volume of $<1\text{ cm}^3$), peak SUV (SUV_{peak}, i.e., the mean of the three highest ^{18}F -FDG contents in three pixels within a volume of $<1\text{ cm}^3$), max SUV (SUV_{max}, i.e., the maximum quantity of ^{18}F -FDG contents in three pixels within a volume of $<1\text{ cm}^3$)²⁰.

2.5. Blood sample collection and determination of cardiometabolic risk factors

Blood samples were taken at baseline after 10 h of fasting¹³. Serum glucose, total cholesterol (TC), high-density lipoprotein-cholesterol (HDL-C), apolipoprotein A1 (APOA1) and B (APOB), triglycerides (TG), as well as liver enzymes, i.e., glutamic pyruvic transaminase (GPT), gamma-glutamyl transferase (GGT), and alkaline phosphatase (ALP) levels, were assessed following standard methods using an AU5832 automated analyzer (Beckman Coulter Inc., Brea, CA, USA) with Beckman Coulter reagents (OSR6521, OSR6116, OSR60118, OSR446410, OSR447730, OSR6507, OSR6520, OSR6204 and OSR6187, respectively). Low-density lipoprotein-cholesterol (LDL-C) was estimated as: [total cholesterol – HDL-C – (TG/5)], with all units in mg/dL²¹. Serum insulin was measured using the Access Ultrasensitive Insulin chemiluminescent immunoassay kit (Beckman Coulter Inc., Brea, CA, USA, 33410). The homeostatic model assessment for insulin resistance index (HOMA index) was calculated as insulin levels ($\mu\text{U}/\text{mL}$) multiplied by glucose levels (mmol/L)/22.5²², whereas the fatty liver index was calculated following standard guidelines²³. C-reactive protein (CRP), complement component C3 (C3), and complement component C4 (C4) concentrations were measured by immunoturbidimetric assays (OSR6299, OSR6159, and OSR6160) using an AU5832 spectrophotometer. Leptin and adiponectin concentrations were measured using the MILLIPLEX MAG Human Adipokine Magnetic Bead Panel 2 and MILLIPLEX MAP Human Adipokine Magnetic Bead Panel 1, respectively (Luminex Corporation, Austin, TX, USA). The metabolic

syndrome prevalence was calculated following the National Cholesterol Education Program Adult Treatment Panel III (ATP III)²⁴ and International Diabetes Federation (IDF) classifications²⁵. An Omron M6 upper arm blood pressure monitor (Omron Healthcare Europe B.V., Hoofddorp, The Netherlands) was used to determine the systolic blood pressure (SBP) and diastolic blood pressure (DBP), with subjects seated and relaxed; measurements were taken at three time points with the mean used in later analyses.

2.6. Classification of metabolically healthy overweight-obese and metabolically unhealthy overweight-obese participants

Overweight or obese individuals were divided into two groups: metabolically healthy overweight-obese (MHOO) and metabolically unhealthy overweight-obese (MUOO) groups. MHOO participants were defined as having a BMI ≥ 25 kg/m² and not presenting any of the following criteria²⁶: (i) serum TG concentration ≥ 150 mg/dL; (ii) serum HDL-C concentration ≤ 40 mg/dL for men and ≤ 50 mg/dL for women; (iii) SBP ≥ 130 mmHg or DBP ≥ 85 mmHg; or (iv) serum glucose concentration ≥ 100 mg/dL. MUOO participants were defined as having a BMI ≥ 25 kg/m² and presenting at least one of the cardiometabolic risk factors mentioned above factors.

2.7. Statistical analysis

Categorical and continuous variables were used to describe the clinical and demographic characteristics of the study participants. Since peak area ratios of the plasma eCBs and their analogues and blood cardiometabolic risk factors did not follow a normal distribution, they were log₁₀ transformed to obtain normal distributions. Data were presented as mean \pm standard deviation unless otherwise stated. Since no sex interaction was observed (all $P > 0.05$), data from both sexes were pooled together for all the statistical analyses unless otherwise stated. Pearson correlations of plasma levels of eCBs and their analogues with body composition and cardiometabolic risk factors were obtained using R (V.3.6.0). Correlation plots were built using the R package 'corrplot'. In separate models, forward stepwise regression analyses were conducted with FBM and VAT as dependent outcomes. The measured plasma eCBs and their analogues and leptin and adiponectin values were introduced as predictors using a 'forward stepwise' procedure. This procedure introduces predictor components step-by-step into the model (if $P < 0.05$) according to the strength of

their association with the dependent outcome. All forward stepwise regression analyses were performed with Statistical Package for the Social Sciences v.22.0 (IBM Corporation, Chicago, IL, USA), with a significance level set at $P < 0.05$. The differences in the plasma levels of eCBs between MHOO and MUOO individuals were assessed using one-way analyses of covariance (ANCOVA), including either sex or VAT as a confounder. Box plots were made using GraphPad Prism software v.9 (GraphPad Software, San Diego, CA, USA).

3. RESULTS

3.1 Characteristics of the study participants and plasma levels of endocannabinoids and their analogues

The characteristics of the study participants are shown in **Table 1**. The LC-MS/MS method enabled the relative quantitation of 14 eCBs and their analogues. Among those, eight metabolites showed RSD values for peak area ratios in QC samples lower than 15%, while six metabolites were detected with RSDs between 15% and 30% in QC samples (**Table 1**). The data quality was confirmed based on the acceptance criteria typically used in metabolomics-based experiments^{27,28}.

3.2 Plasma levels of endocannabinoids and their analogues are positively correlated with adiposity and cardiometabolic risk factors

The plasma levels of AEA, 2-AG, and most of the eCB analogues (i.e., 2-LG, 2-OG, DGLEA, LEA, PEA, POEA, OEA, and SEA) were positively correlated with adiposity (i.e., BMI, waist circumference, FBM, and VAT, **Figure 1**). Notably, POEA showed a negative correlation with LBM ($r = -0.33$, $P < 0.001$) and LMI ($r = -0.29$, $P < 0.001$). DHEA, α -LEA, and PDEA did not significantly correlate with body composition parameters (**Figure 1**). 2-AG and PDEA, but not AEA, showed negative correlations with BAT parameters (i.e., BAT volume and glucose uptake by BAT; all $r \leq -0.19$, $P \leq 0.031$, **Figure 1**).

The plasma levels of AEA, 2-AG, and eCB analogues were positively correlated with cardiometabolic risk factors (**Figure 2**). Both 2-AG and AEA showed positive correlations with the prevalence of metabolic syndrome assessed by ATP III ($r \geq 0.33$, $P < 0.001$, **Figure 2**) and IDF ($r \geq 0.39$, $P < 0.001$, **Figure 2**). Positive correlations were observed between the

eCBs and glucose parameters (i.e., insulin glucose ratio, glucose, insulin, HOMA index), as well as some of the lipid parameters (i.e., TC, LDL-C, APOB, and TG levels) and the fatty liver index (**Figure 2**). Only AEA showed a weak and negative correlation with adiponectin levels ($r=-0.19$, $P=0.035$, **Figure 2**). 2-AG and AEA were not correlated with leptin levels. 2-LG, 2-OG, and most of the NAEs showed positive correlations with the prevalence of metabolic syndrome assessed by ATP III ($r\geq 0.18$, $P<0.038$) and IDF ($r\geq 0.18$, $P<0.012$) (**Figure 2**). 2-LG, 2-OG, and DGLEA were positively correlated with parameters related to insulin resistance (insulin glucose ratio, glucose, insulin, HOMA index; $r\geq 0.17$, $P<0.046$, **Figure 2**). DGLEA, PEA, POEA, OEA, and SEA showed positive correlations with lipid parameters (i.e., TC, LDL-C, APOB, and TG levels; $r\geq 0.18$, $P<0.044$, **Figure 2**). Interestingly, POEA showed positive correlations with both leptin ($r=0.32$, $P<0.001$, **Figure 2**) and adiponectin levels ($r=0.21$, $P<0.02$, **Figure 2**).

Based on the significant correlations observed, we performed stepwise linear regression models to study whether the plasma levels of eCBs and their analogues can improve the prediction of FBM and VAT by classical markers (i.e., leptin and adiponectin). These analyses showed that AEA and POEA improved the prediction of FBM by leptin and adiponectin by 14.2%, and the prediction of VAT by 13.7% (**Table S2**).

3.3 Plasma levels of endocannabinoids and many analogues are higher in metabolically unhealthy compared to metabolically healthy overweight-obese participants

In order to further understand the biological meaning of all correlations observed, we divided the cohort between MHOO ($n=38$) and MUOO ($n=20$) individuals. These analyses showed that these groups were similar in terms of BMI, LMI, and FBM ($p\geq 0.27$); however, MUOO participants showed higher VAT depots than MHOO participants ($p=0.028$, **Table S3**). In addition, we found that MUOO individuals showed higher plasma levels of AEA and 2-AG compared with MHOO (all $\geq 18\%$ difference, $p\leq 0.034$, **Figure 3**). Similarly, the plasma levels of NAEs (i.e., DHEA, LEA, PEA, and OEA) and 2-OG were also higher in MUOO compared with MHOO participants (all $\geq 8\%$ difference, $P\leq 0.045$, **Figure 3**). However, all the significant differences disappeared when VAT was included as a confounder (data not shown).

Table 1. Characteristics of the participants

	N	Total	N	Men	N	Women
Age (years)	136	22.1 (2.2)	45	22.3 (2.3)	91	21.9 (2.2)
<i>Body composition</i>						
Body mass index (kg/m ²)	136	24.9 (4.6)	45	26.8 (5.5)	91	23.9 (3.7)
Lean body mass (kg)	136	41.8 (9.7)	45	52.8 (7.2)	91	36.3 (5.0)
Lean mass index (kg/m ²)	136	14.7 (2.4)	45	17.2 (2.1)	91	13.5 (1.4)
Fat body mass (kg)	136	24.7 (8.8)	45	24.8 (11.0)	91	24.6 (7.5)
Fat mass (%)	136	35.5 (7.6)	45	29.7 (7.6)	91	38.3 (5.9)
Fat mass index (kg/m ²)	136	8.8 (3.0)	45	8.1 (3.6)	91	9.1 (2.7)
Visceral adipose tissue (g)	136	336.4 (174.1)	45	417.9 (175.9)	91	296.1 (159.2)
Waist circumference (cm)	130	81.0 (4.6)	43	89.9 (15.2)	87	76.5 (10.5)
<i>Brown adipose tissue</i>						
BAT volume (mL)	131	68.5 (57.4)	42	78.9 (66.0)	89	63.6 (52.6)
BAT metabolic activity	131	332.9 (328.7)	42	326.8 (327.8)	89	335.8 (331.0)
BAT SUV _{mean}	131	3.7 (1.9)	42	3.2 (1.3)	89	4.0 (2.1)
BAT SUV _{peak}	131	11.1 (8.2)	42	9.9 (7.3)	89	11.6 (8.6)
BAT SUV _{max}	131	12.2 (9.0)	42	10.8 (8.1)	89	12.8 (9.4)
<i>Cardiometabolic risk factors</i>						
Metabolic syndrome ATP III	128	0.5 (0.9)	42	1.0 (1.3)	86	0.2 (0.5)
Metabolic syndrome IDF	128	0.7 (1.1)	42	1.1 (1.5)	86	0.5 (0.7)
Fatty liver index	132	20.4 (25.0)	43	36.9 (32.0)	89	12.5 (15.7)
GTP (IU/L)	131	19.0 (17.5)	43	28.4 (26.8)	88	14.4 (6.7)
GGT (IU/L)	131	19.8 (20.0)	43	29.9 (29.8)	88	14.9 (9.9)
ALP (IU/L)	132	71.3 (18.5)	43	79.3 (19.4)	89	67.5 (16.9)
C-reactive protein (mg/L)	132	2.4 (3.4)	43	2.1 (2.3)	89	2.5 (3.8)
C3 (mg/dL)	132	137.4 (23.8)	43	143.0 (26.2)	89	134.7 (22.2)
C4 (mg/dL)	132	28.7 (8.8)	43	30.3 (9.9)	89	27.9 (8.1)
Insulin glucose ratio	132	14.1 (7.0)	43	14.8 (8.8)	89	13.8 (6.0)
HOMA index	132	1.8 (1.2)	43	2.1 (1.6)	89	1.7 (1.0)
Glucose (mg/dL)	132	87.6 (6.6)	43	88.9 (7.4)	89	87.0 (6.1)
Insulin (μIU/mL)	132	8.3 (4.9)	43	9.1 (6.4)	89	8.0 (4.0)
Total cholesterol (mg/dL)	132	165.1 (32.2)	43	160.1 (30.9)	89	167.6 (32.7)
HDL-C (mg/dL)	132	52.8 (11.0)	43	46.0 (7.4)	89	56.0 (11.0)
LDL-C (mg/dL)	132	96.0 (25.3)	43	96.5 (26.2)	89	95.8 (25.0)
APOA1 (mg/dL)	113	144.7 (27.5)	37	130.0 (16.8)	76	151.9 (28.9)
APOB (mg/dL)	113	69.7 (19.9)	37	72.7 (24.4)	76	68.3 (17.3)
Triglycerides (mg/dL)	132	82.5 (44.6)	43	88.2 (47.2)	89	79.7 (43.2)
Leptin (μg/L)	129	6.2 (4.4)	42	4.4 (4.0)	87	7.1 (4.3)
Adiponectin (mg/L)	127	11.4 (7.9)	42	7.7 (5.2)	85	13.3 (8.3)
Systolic blood pressure (mmHg)	134	116.7 (11.6)	44	125.3 (10.9)	90	112.5 (9.5)
Diastolic blood pressure (mmHg)	134	70.9 (7.6)	44	72.2 (9.2)	90	70.3 (6.7)
<i>Circulating endocannabinoids (peak area ratio)</i>						
AEA	133	0.14 (0.06)	43	0.14 (0.05)	90	0.13 (0.06)
2-AG*	133	0.18 (0.13)	43	0.21 (0.21)	90	0.16 (0.07)
AA	133	64.3 (20.7)	43	61.14 (18.42)	90	65.81 (21.64)
2-LG*	133	0.17 (0.28)	43	0.22 (0.44)	90	0.15 (0.15)
2-OG*	133	0.04 (0.07)	43	0.05 (0.12)	90	0.03 (0.04)
DHEA*	133	0.1 (0.24)	43	0.12 (0.36)	90	0.08 (0.16)
DGLEA*	132	0.21 (0.08)	43	0.2 (0.06)	89	0.21 (0.09)
LEA	133	0.01 (0)	43	0.01 (0)	90	0.01 (0)
α-LEA	133	1.72 (0.27)	43	1.71 (0.22)	90	1.72 (0.29)
PEA	132	0.02 (0.01)	43	0.02 (0.01)	89	0.02 (0.01)
PDEA*	133	0.26 (0.2)	43	0.18 (0.12)	90	0.3 (0.22)
POEA	133	0.68 (0.2)	43	0.65 (0.17)	90	0.69 (0.21)
OEA	133	1.26 (0.22)	43	1.27 (0.21)	90	1.26 (0.23)
SEA	133	0.14 (0.06)	43	0.14 (0.05)	90	0.13 (0.06)

Data are presented as mean (standard deviation). Abbreviations: 2-AG: 2-arachidonoylglycerol; 2-LG:

2-linoleoylglycerol; 2-OG: 2-oleoylglycerol; α -LEA: α -linolenylethanolamine; AA: arachidonic acid; AEA: anandamide; ALP: Alkaline phosphatase; APOA1: apolipoprotein A1; APOB: apolipoprotein; BAT: brown adipose tissue; DGLEA: N-dihomo-gamma-linolenylethanolamine; DHEA: N-docosahexaenoylethanolamine; C3: complement component 3; C4: complement component 4; GGT: gamma-glutamyl transferase; GTP: glutamic pyruvic transaminase; HDL-C: high-density lipoprotein cholesterol; HOMA index: homeostatic model assessment for insulin resistance index; LDL-C: low-density lipoprotein cholesterol; LEA: N-linoleylethanolamine; Metabolic syndrome ATP III: Metabolic syndrome prevalence calculated following the National Cholesterol Education Program Adult Treatment Panel III classification; Metabolic syndrome IDF: Metabolic syndrome prevalence calculated following the International Diabetes Federation (IDF) classification; OEA: N-oleylethanolamine; PEA: N-palmitoylethanolamine; PDEA: N-pentadecanoylethanolamine; POEA: N-palmitoylethanolamine; SEA: N-stearoylethanolamine; SUV: standardized uptake value. * Analytes to be considered with caution, as relative standard deviations were between 15% and 30% in quality control samples.

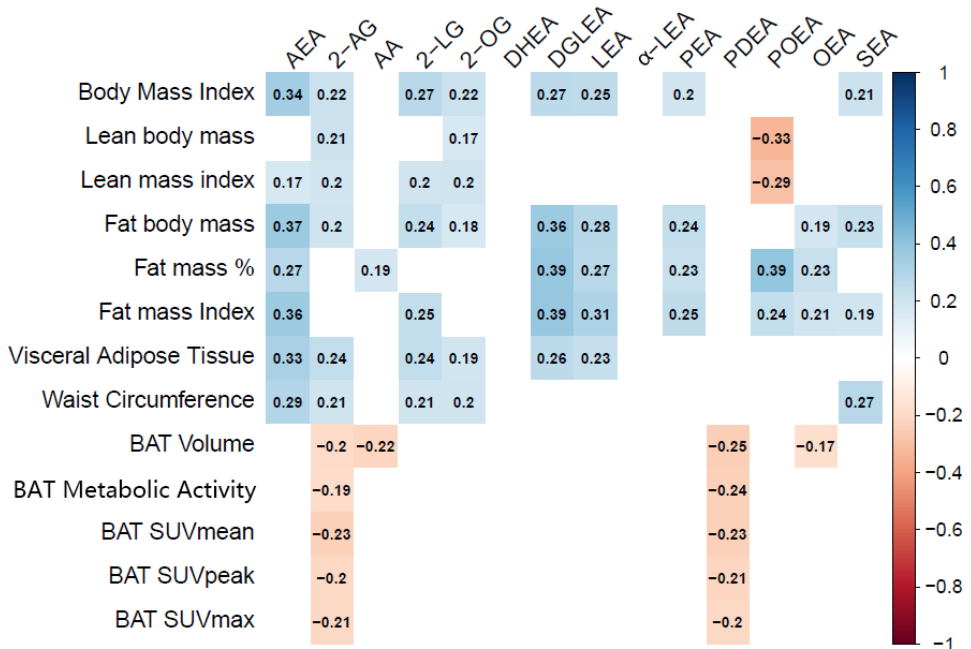


Figure 1. Pearson correlations between plasma levels of endocannabinoids and their analogues with body composition and brown adipose tissue parameters in young and sedentary adults (n=133). Every box represents a statistically significant correlation coefficient (P<0.05), whereas empty spaces represent no statistically significant correlations. Blue and red boxes indicate positive and negative correlations, respectively. 2-AG: 2-arachidonoylglycerol; 2-LG: 2-linoleoylglycerol; 2-OG: 2-oleoylglycerol; α -LEA: N- α -linolenylethanolamine; AA: arachidonic acid; AEA: anandamide; BAT: brown adipose tissue; DGLEA: N-dihomo-gamma-linolenylethanolamine; DHEA: N-docosahexaenoylethanolamine; LEA: N-linoleylethanolamine; OEA: N-oleylethanolamine; PEA: N-palmitoylethanolamine; PDEA: N-pentadecanoylethanolamine; POEA: N-palmitoylethanolamine; SEA: N-stearoylethanolamine; SUV: standardized uptake value.

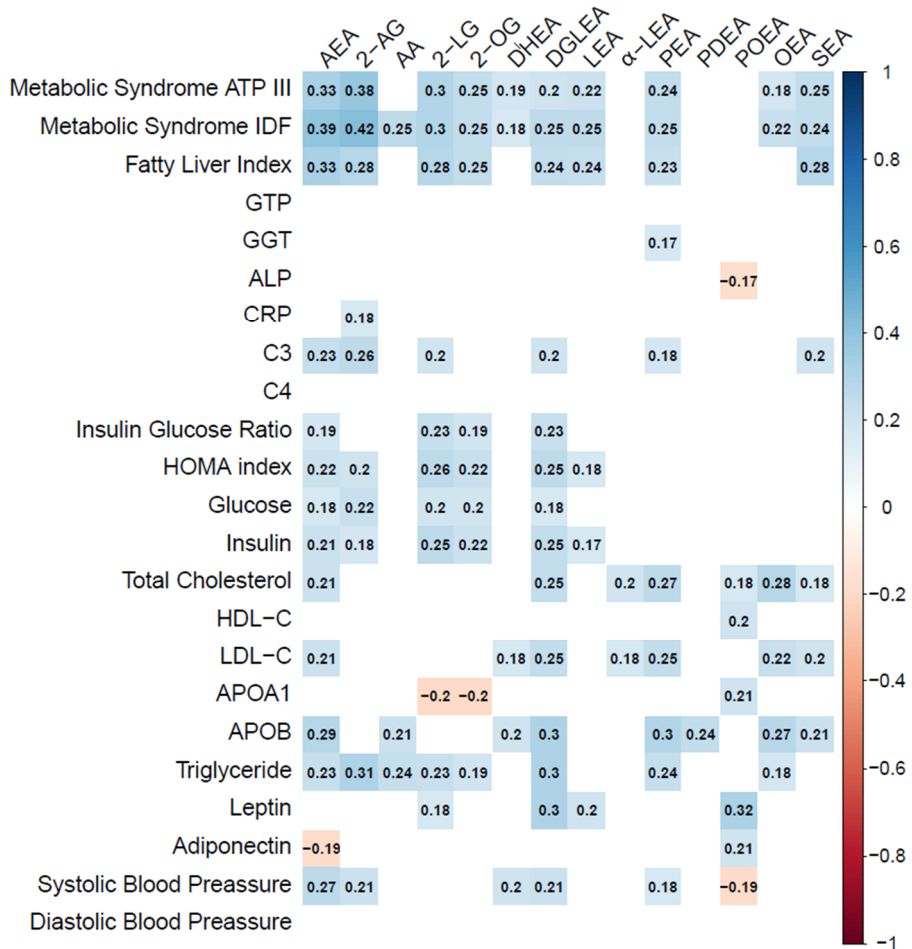


Figure 2. Pearson correlations between plasma levels of endocannabinoids and their analogues with cardiometabolic risk factors in young sedentary adults (n=133). Every box represents a statistically significant correlation coefficient ($P < 0.05$), whereas empty spaces represent no statistically significant correlations. Blue and red boxes indicate positive and negative correlations, respectively. 2-AG: 2-arachidonoylglycerol; 2-LG: 2-linoleoylglycerol; 2-OG: 2-oleoylglycerol; α -LEA: α -linolenoylethanolamine; AA: arachidonic acid; AEA: anandamide; ALP: alkaline phosphatase; APOA1: apolipoprotein A1; APOB: apolipoprotein B; BAT: brown adipose tissue; C3: complement component C3; C4: complement component C4; CRP: C-reactive protein; DGLEA: N-dihomogamma-linolenoylethanolamine; DHEA: N-docosahexaenoylethanolamine; GTP: transaminase; GGT: gamma-glutamyl transferase; HDL-C: high-density lipoprotein cholesterol; HOMA index: homeostatic model assessment for insulin resistance index; LDL-C: low-density lipoprotein cholesterol; LEA: N-linoleoylethanolamine; Metabolic syndrome ATP III: Metabolic syndrome prevalence calculated following the National Cholesterol Education Program Adult Treatment Panel III classification; Metabolic syndrome IDF: Metabolic syndrome prevalence calculated following the International Diabetes Federation (IDF) classification; OEA: N-oleoylethanolamine; PEA: N-palmitoylethanolamine; PDEA: N-pentadecanoylethanolamine; POEA: N-palmitoleoylethanolamine; SEA: N-stearoylethanolamine.

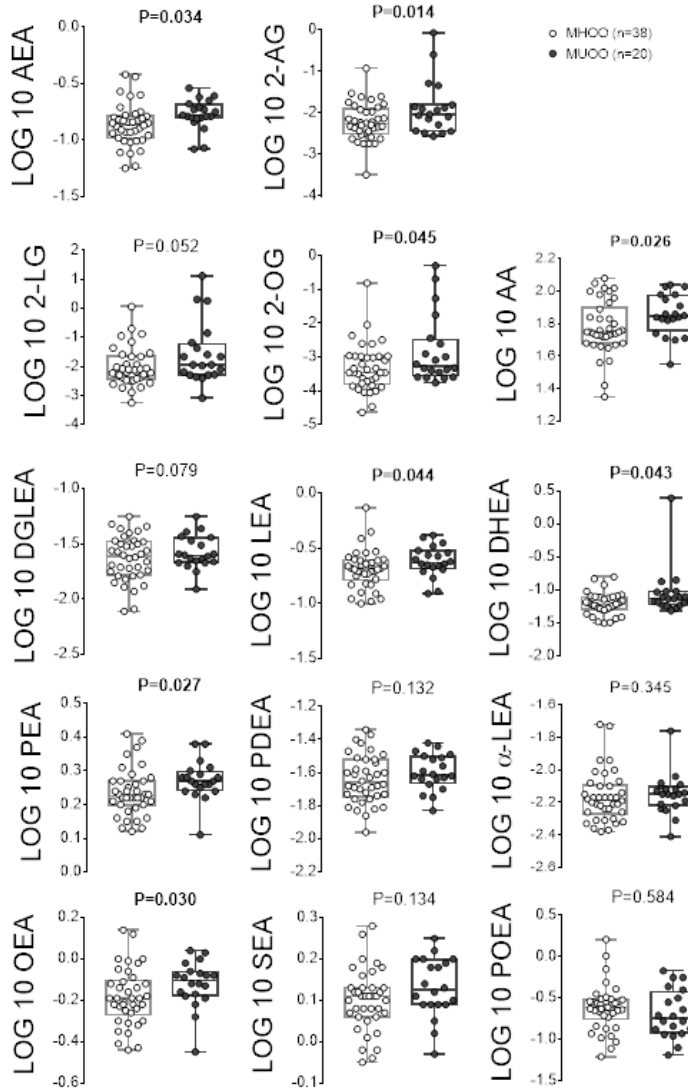


Figure 3. Differences in plasma levels of endocannabinoids and their analogues between metabolically healthy overweight-obese (MHOO) individuals and metabolically unhealthy overweight-obese individuals (MUOO). P values were obtained from one-way analyses of covariance (ANCOVA) and were adjusted for sex. 2-AG: 2-arachidonoylglycerol; 2-LG: 2-linoleoylglycerol; 2-OG: 2-oleoylglycerol; α-LEA: N-α-linolenylethanolamine; AA: arachidonic acid; AEA: anandamide; DGLEA: N-dihomo-gamma-linolenylethanolamine; DHEA: docosahexaenylethanolamine; HOMA: homeostatic model assessment for insulin resistance index; LEA: N-linoleylethanolamine; OEA: N-oleylethanolamine; PEA: N-palmitoylethanolamine; PDEA: N-pentadecanoylethanolamine; POEA: N-palmitoylethanolamine; SEA: N-stearoylethanolamine.

DISCUSSION

In this study, we found that plasma levels of eCBs and their analogues were positively correlated with adiposity and cardiometabolic risk factors in young adults. Moreover, MUOO participants displayed significantly higher plasma levels of eCBs and their analogues than MHOO participants, although these differences disappeared when VAT was included as confounder. These findings show that plasma levels of eCBs and their analogues can predict body composition parameters such as VAT, which suggests that these metabolites may be used as early markers of cardiometabolic risk in young adults.

The positive correlations between plasma levels of eCBs and adiposity might be explained by i) the role of ECS in regulating energy metabolism or ii) the secretion of eCBs and other analogues by white adipose tissue (WAT) and VAT. In the central nervous and digestive systems, elevated eCB levels stimulate food intake and increase food-seeking behavior in mice^{5,29-31}. In human WAT, CB1R activation increases fat storage by stimulating fatty acid uptake, *de novo* lipogenesis, and adipocyte differentiation^{6,32}. Moreover, VAT synthesizes and secretes eCBs into the circulation^{32,33}, which supports the correlation we observed, and in turn, may further stimulate food intake. On the other hand, our results show that 2-AG is negatively correlated with BAT glucose uptake, suggesting that activation of ECS might be related to decreased BAT activity in humans. This is in accordance with a preclinical study in which CB1R blockade increased BAT activity³⁴, which suggests that 2-AG may inhibit BAT activity by binding to CB1R.

We also observed a positive correlation between plasma levels of eCBs and cardiometabolic risk factors, including parameters related to insulin resistance, dyslipidemia, and metabolic syndrome. Similar results have been reported in a clinical study where plasma levels of 2-AG, but not AEA, were positively correlated with cardiometabolic risk factors (i.e., HDL-C, TG, insulin, and glucose levels) in a cohort of 62 middle-aged males (age = 42.2 ± 7.8 years, BMI = 27.4 ± 4.5 kg/m²)⁹. These results are in accordance with a preclinical experiment, where chronic exposure to corticosterone led to an increase of plasma eCBs levels and the development of metabolic syndrome³⁵. Another study in mice revealed that a high-fat diet-induced activation of ECS in liver and WAT to insulin-resistance³⁶. Interestingly, these mice studies reported that higher hepatic and plasma eCB levels, as well

as a higher hepatic expression of eCB synthesis enzymes, are linked to a deteriorated liver function^{37,38}. This deterioration of liver function is attenuated by CB1R deficiency or CB1R inhibition³⁷, suggesting that this deterioration of liver function is mediated by the activation of ECS. At the same time, we did not observe any correlations between plasma eCBs and liver function parameters (i.e., GPT, GGT, and ALP), which could be explained by the relatively young age of our cohort.

Similar to AEA and 2-AG, their analogues (i.e., 2-OG, DHEA, LEA, PEA, and OEA) also showed positive correlations with adiposity parameters and cardiometabolic risk factors. NAEs are produced from N-acyl phosphatidylethanolamines (NAPEs) by NAPE-specific phospholipase D (NAPE-PLD) and catabolized by fatty acid amide hydrolase (FAAH)^{10,37}. Alterations of the metabolic enzymes involved in eCBs metabolism have been observed in adipose tissues from obese individuals^{33,38}, including down-regulation of FAAH that could explain the higher levels of AEA and other NAEs with increased adiposity.

Interestingly, we observed that the plasma levels of eCBs and their analogues were significantly higher in MUOO participants compared with MHOO participants although these differences disappeared when VAT was included as confounder. This result shows that VAT may be a key endocrine organ that could regulate the plasma levels of eCBs and their analogues. Thus, further studies are required to unveil whether individuals with higher eCBs and their analogues levels in the circulation have higher VAT mass, or whether VAT differently contributes to the synthesis of eCBs and their analogues compared to other adipose tissue depots (e.g., subcutaneous adipose tissue).

Strengths and limitations

Most of the eCB analogues, including the unstudied ones like POEA, have been analysed with our LC-MS method. Moreover, our study population size is the largest cohort reporting eCBs and their analogues in combination with BAT parameters so far. This study also has limitations. The area peak ratio but not the absolute plasma concentration of eCBs and their analogues were reported. No causality can be established due to the inherent limitation of all cross-sectional studies. Since we only included young adults, we cannot extrapolate our results to older or unhealthy populations. Finally, the results related to BAT parameters

should be treated with caution, as the method for quantifying BAT volume and activity has limitations, as described elsewhere ^{39,40}.

CONCLUSIONS

The plasma levels of eCBs and their analogues are related to higher levels of adiposity and cardiometabolic risk factors in young adults. Of note, MUOO participants showed higher plasma levels of eCBs and their analogues than their MHOO counterparts, and the differences disappeared when VAT was included as a confounder. Overall, our results suggest that eCBs and their analogues may be used as potential markers for the diagnosis of cardiometabolic risks even in young healthy adults.

Funding

This study was supported by the Spanish Ministry of Economy and Competitiveness via the Fondo de Investigación Sanitaria del Instituto de Salud Carlos III (PI13/01393), and and PTA-12264, Retos de la Sociedad (DEP2016-79512-R) and European Regional Development Funds (ERDF), the Spanish Ministry of Education (FPU16/02828, FPU17/01523 and FPU19/01609), the Fundación Iberoamericana de Nutrición (FINUT), the Redes Temáticas de Investigación Cooperativa RETIC (Red SAMID RD16/0022), the AstraZeneca HealthCare Foundation, the University of Granada Plan Propio de Investigación 2016 -Excellence actions: Unit of Excellence on Exercise and Health (UCEES), the Junta de Andalucía, Consejería de Conocimiento, Investigación y Universidades (ERDF; ref. SOMM17/6107/UGR and DOC 01151), the Fundación Alfonso Martín Escudero, the Netherlands CardioVascular Research Initiative: ‘the Dutch Heart Foundation, Dutch Federation of University Medical Centers, the Netherlands Organization for Health Research and Development and the Royal Netherlands Academy of Sciences’ (CVON2017-20 GENIUS-2) to PCNR, and the Chinese Scholarship Council (CSC, No. 201707060012) to XD.

References

1. Sattar N, Gill JMR, Alazawi W. Improving prevention strategies for cardiometabolic disease. *Nat Med.* 2020;26(3):320-325. doi:10.1038/s41591-020-0786-7
2. Gerdtts E, Regitz-Zagrosek V. Sex differences in cardiometabolic disorders. *Nat Med.* 2019;25(11):1657-1666. doi:10.1038/s41591-019-0643-8
3. Ng M, Fleming T, Robinson M. Erratum: Global, regional, and national prevalence of overweight and obesity in children and adults during 1980-2013: A systematic analysis for the Global Burden of Disease Study 2013 (*Lancet* (2014) 384 (766-781)). *The Lancet.* 2014;384(9945):746. doi:10.1016/S0140-6736(14)61316-7
4. Matsuzawa Y, Funahashi T, Kihara S, Shimomura I. Adiponectin and Metabolic Syndrome. *Arterioscler Thromb Vasc Biol.* 2004;24(1):29-33. doi:10.1161/01.ATV.0000099786.99623.EF
5. Bermudez-Silva FJ, Cardinal P, Cota D. The role of the endocannabinoid system in the neuroendocrine regulation of energy balance. *Journal of Psychopharmacology.* 2012;26(1):114-124. doi:10.1177/0269881111408458
6. Shelke, AR, Roscoe, JA, Morrow, GR, Colman, LK, Banerjee, TK, & Kirshner JJ. Activation of the Peripheral Endocannabinoid System in Human Obesity. *Bone.* 2008;23(1):1-7. doi:10.1038/jid.2014.371
7. Matias, I, Gatta-Cherifi, B, Tabarin, A, Clark, S, Leste-Lasserre, T, Marsicano, G, Piazza, PV, & Cota, D. Endocannabinoids measurement in human Saliva as potential biomarker of obesity. *PLoS One.* 2012;7(7). doi:10.1371/journal.pone.0042399
8. Sipe, J. C, Scott, T. M, Murray, S, Harismendy, O, Simon, GM, Cravatt, BF, & Waalen, J. Biomarkers of endocannabinoid system activation in severe obesity. *PLoS One.* 2010;5(1):1-6. doi:10.1371/journal.pone.0008792
9. Côté, M, Matias, I, Lemieux, I, Petrosino, S, Alméras, N, Després, JP, & di Marzo, V. Circulating endocannabinoid levels, abdominal adiposity and related cardiometabolic risk factors in obese men. *Int J Obes.* 2007;31(4):692-699. doi:10.1038/sj.ijo.0803539
10. Tsuboi, K, Okamoto, Y, Ikematsu, N, Inoue, M, Shimizu, Y, Uyama, T, Wang, J, Deutsch, DG, Burns, MP, Ulloa, NM, Tokumura, A, & Ueda, N. Enzymatic formation of N-acylethanolamines from N-acylethanolamine plasmalogen through N-acylphosphatidylethanolamine-hydrolyzing phospholipase D-dependent and -independent pathways. *Biochim Biophys Acta Mol Cell Biol Lipids.* 2011;1811(10):565-577. doi:10.1016/j.bbalip.2011.07.009
11. Ben-Shabat, S, Fride, E, Sheskin, T, Tamiri, T, Rhee, MH, Vogel, Z, Bisogno, T, de Petrocellis, L, di Marzo, V, & Mechoulam, R. An entourage effect: inactive endogenous fatty acid glycerol esters enhance 2-arachidonoyl-glycerol cannabinoid activity. *Eur J Pharmacol.* 1998;353(1):23-31. doi:10.1016/S0014-2999(98)00392-6
12. Ho WSV, Barrett DA, Randall MD. “Entourage” effects of N-palmitoylethanolamide and N-oleoylethanolamide on vasorelaxation to anandamide occur through TRPV1 receptors. *Br J Pharmacol.* 2008;155(6):837-846. doi:10.1038/bjp.2008.324
13. Sanchez-Delgado, G, Martinez-Tellez, B, Olza, J, Aguilera, CM, Labayen, I, Ortega, FB, Chillón, P, Fernandez-Reguera, C, Alcantara, JMA, Martinez-Avila, WD, Muñoz-Hernandez, V, Acosta, FM, Prados-Ruiz, J, Amaro-Gahete, FJ, Hidalgo-Garcia, L, Rodriguez, L, Ruiz, YAK, Ramirez-Navarro, A, Muros-de Fuentes, MA, García-Rivero Y, Sanchez-Sanchez R, Jimenez JDB, Teresa C, Navarrete S, Lozano R, Brea-Gomez E, Rubio-Lopez J, Ruiz MR, Cano-Nieto A, Llamas-Elvira JM, Rios JAJ, Gil A, Ruiz, JR. Activating brown adipose tissue through exercise (ACTIBATE) in young adults: Rationale, design and methodology. *Contemp Clin Trials.* 2015;45:416-425. doi:10.1016/j.cct.2015.11.004
14. Martinez-Tellez, B, Sanchez-Delgado, G, Garcia-Rivero, Y, Alcantara, JMA, Martinez-Avila, WD, Muñoz-Hernandez, MV, Olza, J, Boon, MR, Rensen, PCN, Llamas-Elvira, JM, & Ruiz, JR. No evidence of brown adipose tissue activation after 24 weeks of supervised exercise training in young sedentary adults in the ACTIBATE randomized controlled trial. *Nature Communications* 2022 13:1. 2022;13(1):1-12. doi:10.1038/s41467-022-32502-x
15. Jurado-Fasoli L, Di X, Kohler I, Osuna-Prieto FJ, Hankemeier T, Krekels E, Harms AC, Yang W, Garcia-Lario Jv, Fernández-Veledo S, Ruiz JR, Rensen PCN & Martinez-Tellez B. Omega-

- 6 and omega-3 oxylipins as potential markers of cardiometabolic risk in young adults Obesity (Silver Spring). 2022;30(1):50-61. doi:10.1002/OBY.23282
16. Jurado-Fasoli, L, Di, X, Sanchez-Delgado, G, Yang, W, Osuna-Prieto, FJ, Ortiz-Alvarez, L, Krekels, E, Harms, AC, Hankemeier, T, Schönke, M, Aguilera, CM, Llamas-Elvira, JM, Kohler, I, Rensen, PCN, Ruiz, JR, & Martinez-Tellez, B. Acute and long-term exercise differently modulate plasma levels of oxylipins, endocannabinoids, and their analogues in young sedentary adults: A sub-study and secondary analyses from the ACTIBATE randomized controlled-trial. EBioMedicine. 2022;85. doi:10.1016/J.EBIOM.2022.104313
 17. Van Der Kloet FM, Bobeldijk I, Verheij ER, Jellema RH. Analytical error reduction using single point calibration for accurate and precise metabolomic phenotyping. J Proteome Res. 2009;8(11):5132-5141. doi:10.1021/pr900499r
 18. Martinez-Tellez, B, Sanchez-Delgado, G, Garcia-Rivero, Y, Alcantara, JMA., Martinez-Avila, WD, Muñoz-Hernandez, MV, Olza, J, Boon, MR, Rensen, PCN, Llamas-Elvira, JM, & Ruiz, JRA new personalized cooling protocol to activate brown adipose tissue in young adults. Front Physiol. 2017;8(NOV):1-10. doi:10.3389/fphys.2017.00863
 19. Chen, KY, Cypess, AM, Laughlin, MR, Haft, CR, Hu, HH, Bredella, MA, Enerbäck, S, Kinahan, PE, Lichtenbelt, WM, Lin, FI, Sunderland, JJ, Virtanen, KA, & Wahl, RL. Brown Adipose Reporting Criteria in Imaging Studies (BARCIST 1.0): Recommendations for Standardized FDG-PET/CT Experiments in Humans. Cell Metab. 2016;24(2):210-222. doi:10.1016/j.cmet.2016.07.014
 20. Martinez-Tellez, B, Nahon, K. J, Sanchez-Delgado, G, Abreu-Vieira, G, Llamas-Elvira, JM, van Velden, FHP, Pereira Arias-Bouda, LM, Rensen, PCN, Boon, MR, & Ruiz, JR. The impact of using BARCIST 1.0 criteria on quantification of BAT volume and activity in three independent cohorts of adults. Sci Rep. 2018;8(1). doi:10.1038/S41598-018-26878-4
 21. William T. Friedewald, Robert I. Levy and DSF. Estimation of the Concentration of Low-Density Lipoprotein Cholesterol in Plasma, Without Use of the Preparative Ultracentrifuge. Clin Chem. 1972;18(6). doi:10.1017/CBO9781107415324.004
 22. C.Matthews J. Instability of brain synaptosomal membrane preparations to repeated ultracentrifugation in isoosmotic density gradients. Life Sci. 1985;37(26):2467-2473. doi:10.1017/CBO9781107415324.004
 23. Bedogni, G, Bellentani, S, Miglioli, L, Masutti, F, Passalacqua, M, Castiglione, A, & Tiribelli, C. The fatty liver index: A simple and accurate predictor of hepatic steatosis in the general population. BMC Gastroenterol. 2006;6:1-7. doi:10.1186/1471-230X-6-33
 24. Lipsy RJ. The National Cholesterol Education Program Adult Treatment Panel III guidelines. Journal of Managed Care Pharmacy. 2003;9(1 Supp A):2-5. doi:10.18553/jmcp.2003.9.s1.2
 25. Carracher AM, Marathe PH, Close KL. International Diabetes Federation 2017. J Diabetes. 2018;10(5):353-356. doi:10.1111/1753-0407.12644
 26. Ortega FB, Lavie CJ, Blair SN. Obesity and Cardiovascular Disease. Circ Res. 2016;118(11):1752-1770. doi:10.1161/CIRCRESAHA.115.306883
 27. Broadhurst, D, Goodacre, R, Reinke, SN, Kuligowski, J, Wilson, ID, Lewis, MR, & Dunn, WB. Guidelines and considerations for the use of system suitability and quality control samples in mass spectrometry assays applied in untargeted clinical metabolomic studies. Metabolomics. 2018;14(6):1-17. doi:10.1007/s11306-018-1367-3
 28. Dunn WB, Wilson ID, Nicholls AW, Broadhurst D. The importance of experimental design and QC samples in large-scale and MS-driven untargeted metabolomic studies of humans. Bioanalysis. 2012;4(18):2249-2264. doi:10.4155/bio.12.204
 29. DiPatrizio NV, Astarita G, Schwartz G, Li X, Piomelli D. Endocannabinoid signal in the gut controls dietary fat intake. Proc Natl Acad Sci U S A. 2011;108(31):12904-12908. doi:10.1073/pnas.1104675108
 30. Soria-Gómez E, Belloccchio L, Reguero L, Lepousez G, Martin C, Bendahmane M, Ruelle S, Remmers F, Desprez T, Matias I, Wiesner T, Cannich A, Nissant A, Wadleigh A, Pape HC, Chiarlone AP, Quarta C, Verrier D, Vincent P, Massa F, Lutz B, Guzmán M, Gurden H, Ferreira G, Lledo PM, Grandes P, Marsicano G. The endocannabinoid system controls food intake via

- olfactory processes. *Nat Neurosci.* 2014;17(3):407-415. doi:10.1038/nn.3647
31. Breunig, E, Manzini, I, Piscitelli, F, Gutermann, B, Di Marzo, V, Schild, D, & Czesnik, D. The endocannabinoid 2-arachidonoyl-glycerol controls odor sensitivity in larvae of *Xenopus laevis*. *Journal of Neuroscience.* 2010;30(26):8965-8973. doi:10.1523/JNEUROSCI.4030-09.2010
 32. van Eenige R, van der Stelt M, Rensen PCN, Kooijman S. Regulation of Adipose Tissue Metabolism by the Endocannabinoid System. *Trends in Endocrinology and Metabolism.* 2018;29(5):326-337. doi:10.1016/j.tem.2018.03.001
 33. Blüher, M, Engeli, S, Klötting, N, Berndt, J, Fasshauer, M, Bátkai, S, Pacher, P, Schön, MR, Jordan, J, & Stumvoll, M. Dysregulation of the peripheral and adipose tissue endocannabinoid system in human abdominal obesity. *Diabetes.* 2006;55(11):3053-3060. doi:10.2337/DB06-0812
 34. Boon, M. R, Kooijman, S, Van Dam, AD, Pelgrom, LR, Berbée, JFP, Visseren, CAR, Van Aggele, RC, Van Den Hoek, AM, Sips, HCM, Lombès, M, Havekes, LM, Tamsma, JT, Guigas, B, Meijer, OC, Jukema, JW, & Rensen, PCN. Peripheral cannabinoid 1 receptor blockade activates brown adipose tissue and diminishes dyslipidemia and obesity. *FASEB Journal.* 2014;28(12):5361-5375. doi:10.1096/fj.13-247643
 35. Bowles, NP, Karatsoreos, IN, Li, X, Vemuri, VK, Wood, JA, Li, Z, Tamashiro, K, Schwartz, GJ, Makriyannis, AM, Kunos, G, Hillard, CJ, McEwen, BS, & Hill, MN. A peripheral endocannabinoid mechanism contributes to glucocorticoid-mediated metabolic syndrome. *Proc Natl Acad Sci U S A.* 2015;112(1):285-290. doi:10.1073/pnas.1421420112
 36. Bartelt, A, Orlando, P, Mele, C, Ligresti, A, Toedter, K, Scheja, L, Heeren, J, & Di Marzo, V. Altered endocannabinoid signalling after a high-fat diet in Apoe ^{-/-} mice: Relevance to adipose tissue inflammation, hepatic steatosis and insulin resistance. *Diabetologia.* 2011;54(11):2900-2910. doi:10.1007/s00125-011-2274-6
 37. Muccioli GG. Endocannabinoid biosynthesis and inactivation, from simple to complex. *Drug Discov Today.* 2010;15(11-12):474-483. doi:10.1016/j.drudis.2010.03.007
 38. Zhang, Y, Sonnenberg, GE, Baye, TM, Littrell, J, Gunnell, J, DeLaForest, A, MacKinney, E, Hillard, CJ, Kissebah, AH, Olivier, M, & Wilke, RA. Obesity-related dyslipidemia associated with FAAH, independent of insulin response, in multigenerational families of Northern European descent. *Pharmacogenomics.* 2009;10(12):1929-1939. doi:10.2217/pgs.09.122
 39. Carpentier AC, Blondin DP, Virtanen KA, Richard D, Haman F, Turcotte ÉE. Brown Adipose Tissue Energy Metabolism in Humans. *Front Endocrinol (Lausanne).* 2018;9:447. doi:10.3389/fendo.2018.00447
 40. Schilperoort M, Hoeke G, Kooijman S, Rensen PCN. Relevance of lipid metabolism for brown fat visualization and quantification. *Curr Opin Lipidol.* 2016;27(3):242-248. doi:10.1097/MOL.0000000000000296

SUPPLEMENTARY MATERIALS

1. Determination of circulating endocannabinoids and endocannabinoid analogues

Endocannabinoids (eCBs), i.e., anandamide (AEA) and 2-arachidonylglycerol (2-AG), and eCB analogues, i.e., 2-linoleoylglycerol (2-LG), 2-oleoylglycerol (2-OG), α -linolenylethanolamine (α -LEA), dihomo- γ -linolenylethanolamine (DGLEA), docosahexaenylethanolamine (DHEA), linoleylethanolamine (LEA), oleylethanolamine (OEA), palmitoylethanolamine (PEA), pentadecanylethanolamine (PDEA), palmitoleylethanolamine (POEA), and stearoylethanolamine (SEA), together with arachidonic acid (AA) were assessed in plasma samples using liquid chromatography – tandem mass spectrometry (LC-MS/MS).

The acyl-glycerols are biologically present under two isomeric forms, namely, 1-AG and 2-AG, 1-LG and 2-LG, as well as 1-OG and 2-OG, respectively. For each isomer pair, a baseline separation was obtained between the two isomers with the developed LC-MS/MS method, as illustrated in **Fig. S1**. However, isomeric conversion due to acyl transformation of the 2-isomer into 1-isomer after sampling is a known mechanism, notably reported for 2-AG¹. Since this conversion could not be experimentally controlled, we summed the peak areas of both isomers 1-AG and 2-AG before calculating the peak area ratio and labelled the isomer pair “2-AG”. The same strategy has been applied for the isomer pairs 1-LG and 2-LG as well as 1-OG and 2-OG, which were labelled “2-LG” and “2-OG”, respectively. Blank effects, corresponding to the signal observed for blank samples, were below 10% for all metabolites except PEA and SEA. The latter were included for further data analysis after blank subtraction, as additional experiments confirmed the reproducibility of the blank signal independent of the solvent batch.

1.1. Sample preparation

The sample preparation, except the evaporation step, was carried out under ice-cold conditions until LC-MS/MS analysis to prevent analyte degradation. eCBs and eCB analogues were extracted using liquid-liquid extraction. Before the extraction, 5 μ L of an antioxidant solution composed of 0.4 mg/mL of butylated hydroxytoluene (BHT) and 10 μ L of a standard internal mixture containing the isotopically-labelled analogues were added to 150 μ L of thawed plasma samples. Then, 150 μ L of a buffer solution composed of 0.2 M citric acid and 0.1 M disodium hydrogen phosphate at pH 4.5 were added to the samples. One mL of the extraction solution composed of butanol (BuOH) and methyl-tert-butylether

(MTBE) in a ratio 50:50 (v/v) was then added before agitation for 5 min using a bullet blender and centrifugation at 16,000g for 10 min at 4°C. The organic supernatant (900 µL) was collected and evaporated to dryness using a SpeedVac under room temperature. The dry residues were then reconstituted in 50 µL of an ice-cold solution of methanol (MeOH) and acetonitrile (ACN) 70:30 (v/v), prior to agitation (5 min) and centrifugation at 16,000g for 10 min at. Finally, 40 µL of the supernatant was transferred into a glass vial for further LC-MS/MS analysis.

1.2. Liquid chromatography – tandem mass spectrometry

Relative quantitation of eCBs and their analogues was carried out using a SCIEX QTRAP® LC-ESI-MS/MS System (SCIEX, Framingham, Massachusetts, USA). The separation was performed using a BEH C18 column (50 mm × 2.1 mm, 1.7 µm) from Waters Technologies (Milford, MA, USA) maintained at 40 °C. The mobile phase was composed of 0.1% acetic acid in water (A), MeCN/0.1% acetic acid in MeOH (90:10, v/v, B), and 0.1% acetic acid in isopropanol (C). The gradient was the following: starting conditions 20% B and 1% C; increase of B from 20% to 26% between 0.75 min and 0.95 min; increase of B from 26% to 34% between 0.95 min and 6 min; increase of B from 34% to 40% between 6 min and 8 min; increase of B from 40% to 54% between 8 min and 10 min; increase of B from 54% to 56% between 10 min and 12 min; increase of C from 1% to 3% between 11 min to 12 min; increase of B from 56% to 78% between 12 min and 13 min; increase of C from 3% to 6% between 12 min to 13 min; increase of B from 78% to 85% between 13 min and 14 min; increase of C from 6% to 15% between 13 min to 14 min; conditions kept for 0.5 min prior to returning to initial conditions at 14.8 min and re-equilibration for 1.2 min. The flow rate was 0.7 mL/min. The sample injection volume was 10 µL, preceded by the injection of 20 µL of mobile phase A as stacking solution to improve peak shape and increase sensitivity. Electrospray ionization (ESI)-MS acquisition was carried out in negative mode, with the following ESI parameters: source temperature, 600°C; Gas 1 (nebulizer gas), 50 L/min; Gas 2 (heater gas), 50 L/min; curtain gas, 30 L/min; collision gas, medium; ion spray voltage, 4500 V for positive and -4500 V for negative. Selected reaction monitoring (SRM) was used for data acquisition.

1.3. Data pre-processing

Peak detection and integration were carried out using SCIEX OS software. The ratio of the

analyte peak area to the peak area of the corresponding isotopically-labelled internal standard referred to as the *peak area ratio* was used for further data analysis. Quality control (QC) samples were prepared using plasma samples from healthy subjects and prepared simultaneously as the study samples. QC samples were regularly injected during the measurements and used to evaluate the data quality, including blank effect, retention time shifts, and peak area ratios, as well as correct for between-batch variations using the in-house developed mzQuality workflow (available at <http://www.mzQuality.nl>)². Relative standard deviations (RSDs) were calculated for each internal standard and analyte present in the QC samples. Metabolites with RSDs $\leq 15\%$ were included in further data analyses. Metabolites showing RSDs higher than 30% on peak area ratios in QC samples were excluded. Metabolites with $15\% \leq \text{RSDs} < 30\%$ were marked and should be interpreted with caution.

References

1. Martin JB. The Equilibrium between Symmetrical and Unsymmetrical Monoglycerides and Determination of Total Monoglycerides. *Journal of the American Chemical Society*. 1953;75(22):5483-5486. doi:10.1021/ja01118a005
2. Van Der Kloet FM, Bobeldijk I, Verheij ER, Jellema RH. Analytical error reduction using single point calibration for accurate and precise metabolomic phenotyping. *Journal of Proteome Research*. 2009;8(11):5132-5141. doi:10.1021/pr900499r

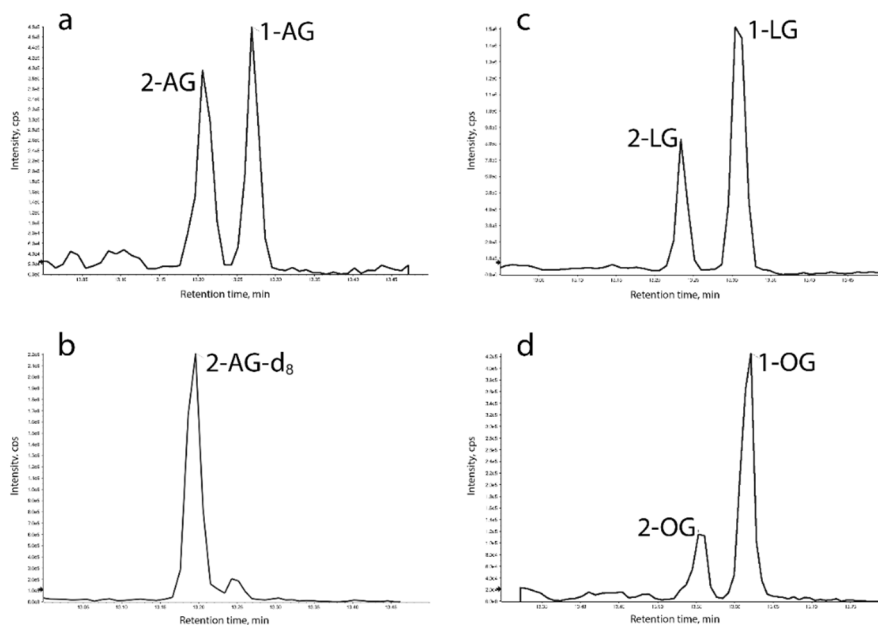


Figure S1. Chromatograms were obtained with the analysis of acyl-glycerols using LC-MS/MS. A) separation between 2-AG and 1-AG. However, due to acyl migration, the sum of the two peaks areas was used for further data analysis. This strategy was also applied to 2-OG (c) and 2-LG (d). 2-AG- d_8 (deuterated form of 2-AG) was used as the internal standard for all the acyl-glycerols. 2-AG: 2-arachidonoylglycerol; 1-AG: 1-arachidonoylglycerol; 2-AG- d_8 : 2-arachidonoylglycerol- d_8 ; 2-LG: 2-linoleoylglycerol; 1-LG: 1-linoleoylglycerol; 2-OG: 2-oleoylglycerol; 1-OG: 1-oleoylglycerol.

Table S1. List of internal standards.

Abbreviation	Name (International Union of Pure and Applied Chemistry, IUPAC)
d8-2-AG	2-(5Z,8Z,11Z,14Z-eicosatetraenoyl)-sn-glycerol- d_8
d8-AEA	N-(5Z,8Z,11Z,14Z-eicosatetraenoyl)-ethanolamine- d_8
d4-DHEA	N-(4Z,7Z,10Z,13Z,16Z,19Z-docosahexaenoyl)-ethanolamine- d_4
d4-LEA	N-(9Z,12Z-octadecadienoyl)-ethanolamine- d_4
d4-OEA	N-(9Z-octadecenoyl)-ethanolamine- d_4
d4-PEA	N-hexadecanoyl-ethanolamine- d_4
d3-SEA	N-(Octadecanoyl)-ethanolamine- d_3

2-AG: 2-arachidonoylglycerol; AEA: anandamide; DHEA: N-docosahexaenoyl ethanolamine; LEA: N-linoleoyl ethanolamine; OEA: N-oleoyl ethanolamine; PEA: N-palmitoyl ethanolamine; SEA: N-stearoyl ethanolamine.

Table S2. Results from forward stepwise regression models assessing the independent association of the predictors with body composition parameters in young healthy adults.

FAT BODY MASS (kg) (n=121)									
	β	B	95% CI		P (coefficients)	R ²	R ² change	F Change	P (model)
Step 1						0.432	-	90.446	<0.001
Leptin	16.285	1.712	12.895	, 19.676	<0.001				
Step 2						0.495	0.063	16.949	<0.001
Leptin	15.370	1.623	12.155	, 18.584	<0.001				
AEA	15.459	3.755	8.023	, 22.895	<0.001				
Step 3						0.574	0.079	22.875	<0.001
Leptin	17.367	1.548	14.301	, 20.434	<0.001				
AEA	27.456	4.265	19.010	, 35.902	<0.001				
POEA	-11.504	2.405	-16.268	, -6.740	<0.001				
Step 4						0.585	0.011	4.050	<0.001
Leptin	16.975	1.541	13.923	, 20.027	<0.001				
AEA	35.755	5.893	24.083	, 47.427	<0.001				
POEA	-8.720	2.748	-14.163	, -3.277	0.002				
OEA	-18.012	8.950	-35.738	, -0.286	0.046				
VISCERAL ADIPOSE TISSUE (g) (n=121)									
Step 1						0.180	-	26.133	<0.001
Adiponectin	-265.702	-0.424	-368.619	, -162.786	<0.001				
Step 2						0.308	0.128	21.746	<0.001
Adiponectin	-246.583	-0.394	-341.908	, -151.258	<0.001				
Leptin	175.509	0.358	100.978	, 250.040	<0.001				
Step 3						0.369	0.061	11.354	<0.001
Adiponectin	-219.727	-0.351	-312.488	, -126.967	<0.001				
Leptin	160.290	0.327	88.265	, 232.316	<0.001				
AEA	287.101	0.254	118.357	, 455.845	0.001				
Step 4						0.445	0.076	15.990	<0.001
Adiponectin	-137.186	-0.219	-233.623	, -40.748	0.006				
Leptin	206.537	0.422	134.955	, 278.119	<0.001				
AEA	566.500	0.500	355.796	, 777.205	<0.001				
POEA	-243.414	-0.395	-363.978	, -122.850	<0.001				
Step 5						0.467	0.021	4.591	<0.001
Adiponectin	-145.149	-0.232	-240.421	, -49.877	0.003				
Leptin	200.508	0.410	129.782	, 271.234	<0.001				
AEA	510.491	0.451	296.593	, 724.388	<0.001				
POEA	-231.377	-0.376	-350.648	, -112.106	<0.001				
2-AG	52.589	0.151	3.973	, 101.206	0.034				

β : standardized regression coefficient; B: unstandardized regression coefficient; CI: confidence interval; R²: adjusted coefficient of determination. expressing the percentual variability of the dependent variable explained by each model; R² change: additional percentual variability explained by the model due to the inclusion of new metabolites. AEA: anandamide; 2-AG: 2-arachidonoylglycerol; OEA: N-oleoylethanolamine; POEA: N-palmitoleoylethanolamine.

Table S3. Descriptive characteristics of metabolically healthy overweight-obese (MHOO) and metabolically unhealthy overweight-obese (MUOO) participants.

	n (%) men	MHOO	n (%) women	MUOO	P
Age (years-old)	39 (28.2)	22.1 ± 0.4	21 (71.4)	23.1 ± 0.5	0.127
Body mass index (kg/m ²)	39	28.9 ± 0.5	21	30.3 ± 0.7	0.270
Lean mass index (kg/m ²)	38 (26.3)	46.9 ± 9.2	19 (73.7)	47.7 ± 12.9	0.629
Visceral adipose tissue (g)	38	468.9 ± 23.6	19	564.3 ± 33.1	0.028
Fat body mass (kg)	38	32.7 ± 12.4	19	34.6 ± 17.4	0.400
Glucose (mg/dL)	39	87.1 ± 1.1	21	94.7 ± 1.6	<0.001
Insulin (μU/mL)	39	9.5 ± 1.1	21	15.2 ± 1.5	0.010
HOMA index	39	2.1 ± 0.3	21	3.7 ± 0.4	0.008
High-density lipoprotein cholesterol (mg/dL)	39	49.9 ± 1.6	21	46.6 ± 2.3	0.271
Low-density lipoprotein cholesterol (mg/dL)	39	92.7 ± 4.7	21	112.9 ± 6.5	0.018
Total cholesterol (mg/dL)	39	156.2 ± 5.9	21	186.2 ± 8.3	0.007
Triglycerides (mg/dL)	39	65.2 ± 9.9	21	162.1 ± 13.9	<0.001
Systolic blood pressure (mmHg)	38 (26.3)	120.5 ± 1.9	21	129.5 ± 2.5	0.008
Diastolic blood pressure (mmHg)	38	69.2 ± 1.2	21	75.1 ± 1.7	0.013

Data are means and standard mean error. P values from analyses of covariance adjusting by sex.

HOMA: homeostatic model assessment for insulin resistance index.